Characterization of Flow Lines Generated by Pressurized Sand Filter Underdrains

Marcio Mesquita [*a], Roberto Testezlaf [b], Fabio P. de Deus[c], Leonardo M. da Rosa[d]

[a] Universidade Federal de Goiás, Goiânia-GO, Brazil
[b] Universidade Estadual de Campinas, Campinas-SP, Brazil
[c] Universidade Federal de Lavras, Lavras-MG, Brazil
[d] Universidade Regional de Blumenau, Blumenau-SC, Brazil

marcio.mesquita@ufg.br

The physical particles filtration, inorganic and organic, is an important action in the irrigation water treatment, preventing emitters clogging, the main operational problem in localized irrigation. Sand filters have better particles removal than screen and discs filters. These equipments have two operation fundamental processes, filtration and backwashing. During these processes the streamlines homogeneity and profile are fundamental parameters to obtain the effectiveness and efficiency of the retention and detachment of impurities, respectively, filtration and backwashing. The purpose of this study was to identify the profile and homogeneity of distribution of fluxes lines and characterizing the trend of flow during the filtration and backwash processes, for different underdrains types (nozzle) used in pressurized sand filters. A Computational Fluid Dynamics (CFD) model was developed further to simulate and analyze the hydrodynamic of the flow in the virtual module configured with three nozzle models, one cylindrical and other conical type, commercially available, and other modified of the conical type, named as "cuca". The results have shown that the commercial models, (cylindrical and conical), provides uneven distribution flow lines and it was observed flux stagnation points, ie., there was no uniform fluid distribution in area of the actuation of the accessory, in flow directions ascending and descending. It phenomenon wasn't identified for optimized drain (cuca). The modified drain presented greater distribution homogeneity of the flow lines and, consequently, the potential to maximize the removal and detachment efficiency of inorganic and organic particles.
Keywords: numerical simulation, localized irrigation, porous media, filtering, backwash, CFD.

1. Introduction

Pressurized sand filters are equipment used in physical treatment of irrigation water, stand out in relation to the others (screen and disc filters) for their superior performance in the retention of organic particles and algae, due to their ability to collect, by adhesion, the impurities particles by the passage of the affluent along the depth of the filter layer (Testezlaf et al. 2014).

In the structure of these equipments there are two internal auxiliary elements, diffuser plate and underdrains (nozzle), responsible for the hydrodynamics of flow during the filtration and backwashing processes. The diffuser plate is allocated at the top of the filter, near the water inlet pipe in the filtration process, and is responsible for avoiding the direct collision of the drained water, reducing the kinetic energy of flow, as well as providing the distribution of the water on the surface of the filter layer evenly and perpendicular to the surface (Mesquita et al. 2012). The nozzles are allocated at the bottom of the filter, near the outlet pipeline, responsible for conducting the filtered water (effluent) to irrigation system during the filtration process, and for evenly distributing the reverse flow water, promoting bed washing porous media (backwash) (Mesquita et al. 2012; de Deus et al. 2016). The authors recommend the adequacy of the structural projects of these components to improve their hydrodynamic behavior. Burt (2010) reinforces this observation by indicating that different nozzle (slots, geometric format, effective area and drainage system arrangement) promote different values of head loss.

The computational fluid dynamics (CFD) technique is used in different analyzes involving fluid flow is defined by Fortuna (2000) as the area of scientific computation that studies numerical methods for the simulation of phenomena involving fluid mechanic with or without heat exchange, using numerical method of elements or finite volumes. The use of this computational technique in the hydrodynamic evaluation of the flow in pressurized sand filters allows to modify the internal structures of the equipment correctly.

The purpose of this study was to identify the profile and homogeneity of distribution of fluxes lines and characterizing the trend of flow during the filtration and backwash processes, for different types of underdrains (nozzle) used in pressurized sand filters. A Computational Fluid Dynamics (CFD) model was developed further to simulate and analyze the hydrodynamic of the flow in the virtual module configured with three nozzle models, one cylindrical and other conical type, commercially available, and other modified of the conical type, named as "cuca".

2. Materials and methods

The CFD was used to simulate the hydrodynamic flow in three nozzle models, one cylindrical and other conical type, marketed in Brazil, and other modified of the conical type, known as "cuca", named F1, F2 and F3, in a virtual module, Figure 1,.
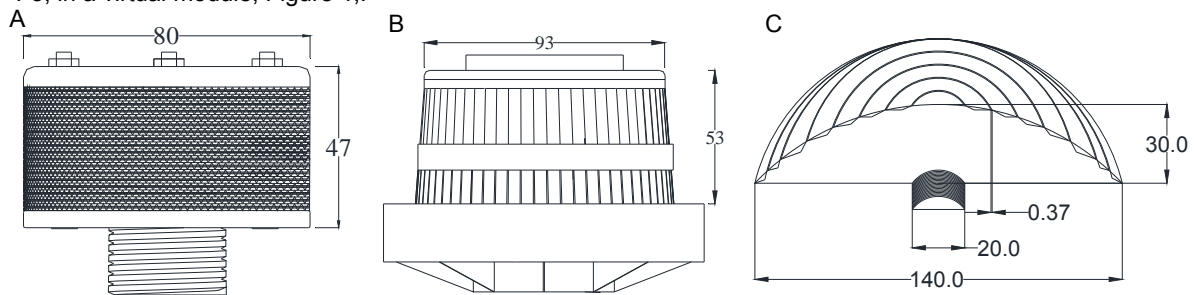

Figure 1: Scheme of evaluated underdrain system, [A] cylindrical nozzle (F1), [B] conical nozzle (F2) and modified conical nozzle (F3) [C]. (units mm).

The virtual module, graphical representation of physical equipment, was designed with structural simplifications when compared to the actual model, Figure 2A. It was considered porous media of 20 cm in height and 30 cm in diameter. These modifications were implanted to isolate the effect caused specifically by the nozzle and, consequently, to isolate the effect of the interactions of any drainage system. As a function of the fluid flow direction, ascending and descending, the input and output domain also varied.
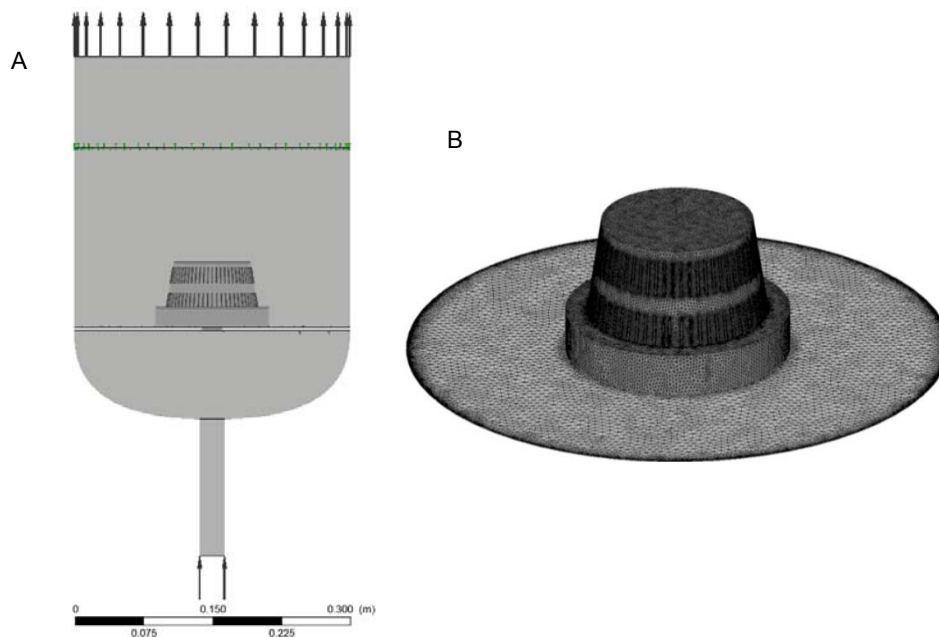

Figure 2: Scheme of evaluated virtual module. [A] boundary conditions. [B] Scheme of mesh.

Tetrahedrons were the mesh model used to represent the volumes. The choice of this mesh model was due the difficulty in generating structured mesh in the sand filters due to the complexity of the structural design of the equipment. There was a refinement of the elements in the nozzle in function of the characteristics and reduced dimensions of the water inlet slots, Figure 2B. Mesh independence studies were performed to ensure that the computed results were independent of the chosen mesh. A total number of 1.5×10^6 elements was used to discretize the section of sand filter.

Considering the equipment operating conditions, the model set up used a steady state simulation, viscous and incompressible Newtonian fluid, isothermal conditions at 25 $^{\circ}$C, establishing the use of transport equations, mass and momentum conservation, and single-phase approach. The solver used was the CFX-ANSYS, parameterized for interpolation of double precision values in high resolution and first order. The physical properties of the fluid were: temperature of 25 $^{\circ}$C, fluid density of 997 kg m^{-3}, fluid viscosity of 1.003×10^{-3} Pa s. The boundary conditions used were: smooth and non-slip wall, output pressure of 50 kPa, turbulent intensity of 1%, Root Mean Square of 1.0×10^{-4}, number of interactions of $300 \leq N_i \leq 3000$.

The input velocity for the upstream flow, coincident with the backwash process, the values adopted were 0.5; 1.5; and 2.5 m s^{-1}. However, in the simulations with downstream flow, coincident to the filtration process, the velocity values were 0.05; 0.15; and 0.25 m s^{-1}, a simplification adopted by considering that the fluid flows inside the equipment with a smaller velocity than in the pipes according to their diameters, based on the principle of conservation of mass, these new values were determined. As the sand filters work under turbulent flow conditions, and given the impossibility, in this case, of obtaining a direct result from the Navier-Stokes equations, the turbulent phenomena were modeled using the Reynolds Averaged Navier-Stokes approach, with standard k-epsilon turbulence model.

The porous media effect on the fluid flow is expressed by eq. (1, 2 e 3).

$$S_i = \left(\frac{\mu}{K_{Perm}} v_i + K_{Loss} \frac{1}{2} \rho |v| v_i \right) \ for \ i = x, y, z \tag{1}$$

$$K_{Perm} = \frac{d_{10}^2}{150} \frac{\varepsilon_l^3}{(1-\varepsilon)^2} \tag{2}$$

$$K_{Loss} = \frac{3,5}{d_{10}} \frac{(1-\varepsilon)}{\varepsilon^3} \tag{3}$$

Where K_{Perm} e K_{Loss} are coefficients of losses by permeability and inertial resistance, respectively, d_{10} effective pore diameter, ε porous media porosity, (v) superficial velocity (m s^{-1}).

These equations consider a loss term caused by viscous effects and another by inertia (ANSYS-CFX, 2009), and was adjusted to a porous media porosity (ε) of 0.43 or 43% and effective pore diameter (d_{10}) of 0.51mm. Arbat et al. (2011) simulating sand filters and using the FLUENT source code, confirmed the significance of this mathematical model in representing the hydraulic behavior of the water flow in porous media.

For the analysis of the results of the flow characterization simulations in the nozzles, velocity contours were plotted in vertical plane axis xy of the virtual module, highlighting the region near the accessory, making it possible to observe the vector fields in this region.

3. Results and discussion

Figures 3 and 4 show the velocity distribution contours obtained in the CFD simulations along a vertical plane, axis xy, under water flows directions coincident with filtration and backwash modes, respectively. These maps highlight the velocity vectors in the direction y, which characterize the affluent streamlines and trajectory in downward direction being possible to observe the operation effective region of each nozzle and the contact areas between drain and filter layer.

When evaluating the flow caused by the cylindrical nozzle it is possible to observe that this geometry provided the formation of stagnation zones, that is, a region where there is no effective flow of current lines, highlighted by dashed lines in the equipment upper part. This behavior was observed by Santos et al. (2013) when testing this cylindrical nozzle model, using wind tunnel methodology, and observed that in the same region there was a point that caused dispersion of the fluid by diverting the trajectory from the smoke to the contour drain region. The conical model had the same effect, due to the areas, at the top and sides, without no slots for fluid

flow. The designs of these two drain models favor drainage on the side of the drain, excluding the top and reducing the area available to the fluid flow.

Santos et al. (2013), still claim that the flow lines dispersion effect in the upper part of the drains can provide an increase in the filtration process pressure loss. In addition, these nozzle model cause uneven flow along the drain, intensifying the flow in the lower part and reducing the efficiency total area of the accessory.
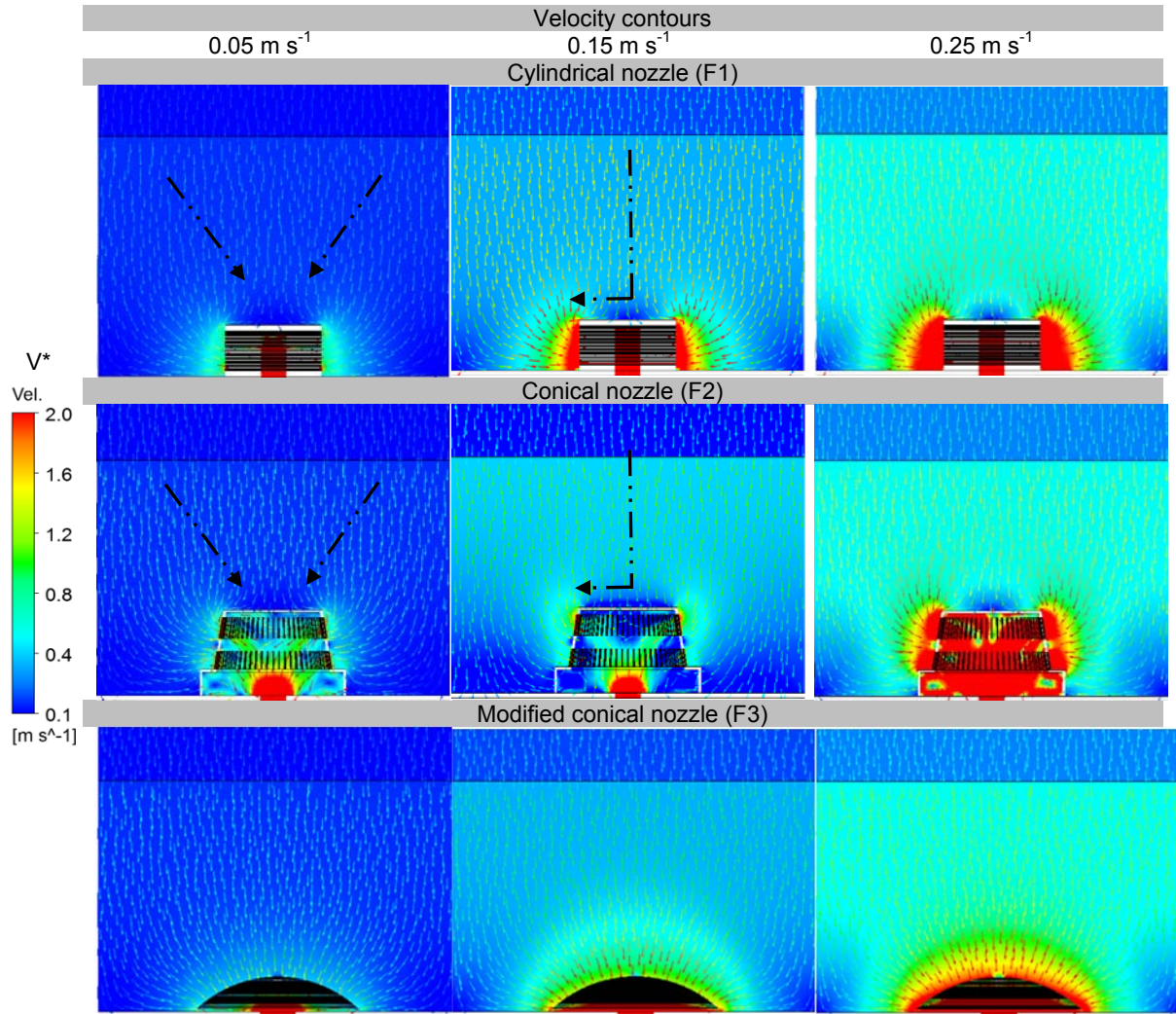

Figure 3: Contour plots of velocity vectors in the direction coincident with the filtration process. Where: [V*] velocity vectors legend

When analyzing the flow profile of the modified nozzle, it was observed that most the flow lines during the downstream process (filtration) are perpendicular to the drain, which reduces the potential for turbulence in the slots inlet, reducing the pressure loss effect. It is also possible to observe that the whole drain area is effectively used, presenting no stagnation flow areas.

In Figure 4 it can be observed that the flow characteristics in cylindrical and conical model were similar to the phenomena found during the downward simulations, with stagnation points forming at the top of the drains and intensification at the sides of the accessory, for the, agreeing with the results found by Santos et al. (2013). These authors suggest that this behavior implies a greater pressure loss in the system, due to the longer path of the line trajectories, in contrast a solely vertical movement of these lines.

Salcedo et al. (2011) commented that this behavior can determine limitations in the fluidized of the porous media during backwash process, becoming more evident when using lower flow velocities. The authors further emphasize that the increase in flow velocity values produces streamlines more quickly to the verticalization, which can generate an uneven arrangement of the filter material, due to the processes that precede the bed fluidization, as the state of bubbling bed, which can be transposed more quickly. Additionally, it is possible to infer that in the projection of these stagnation zones there will not be a flow with significant velocity to provide

the effective movement of the filter bed which will not cause the bed fluidization, allowing the formation of aggregates (accumulations of strongly adherent mixtures of impurity with filtering material). This effect leads to an increase in internal pressure and reduce the effective filtration area in the successive cycles after the backwash processes. Addition it can reduce consequently the removal efficiency due to the increase in interstitial velocity, which will carry impurities already adhered in the sand grains of sand to the irrigation system.
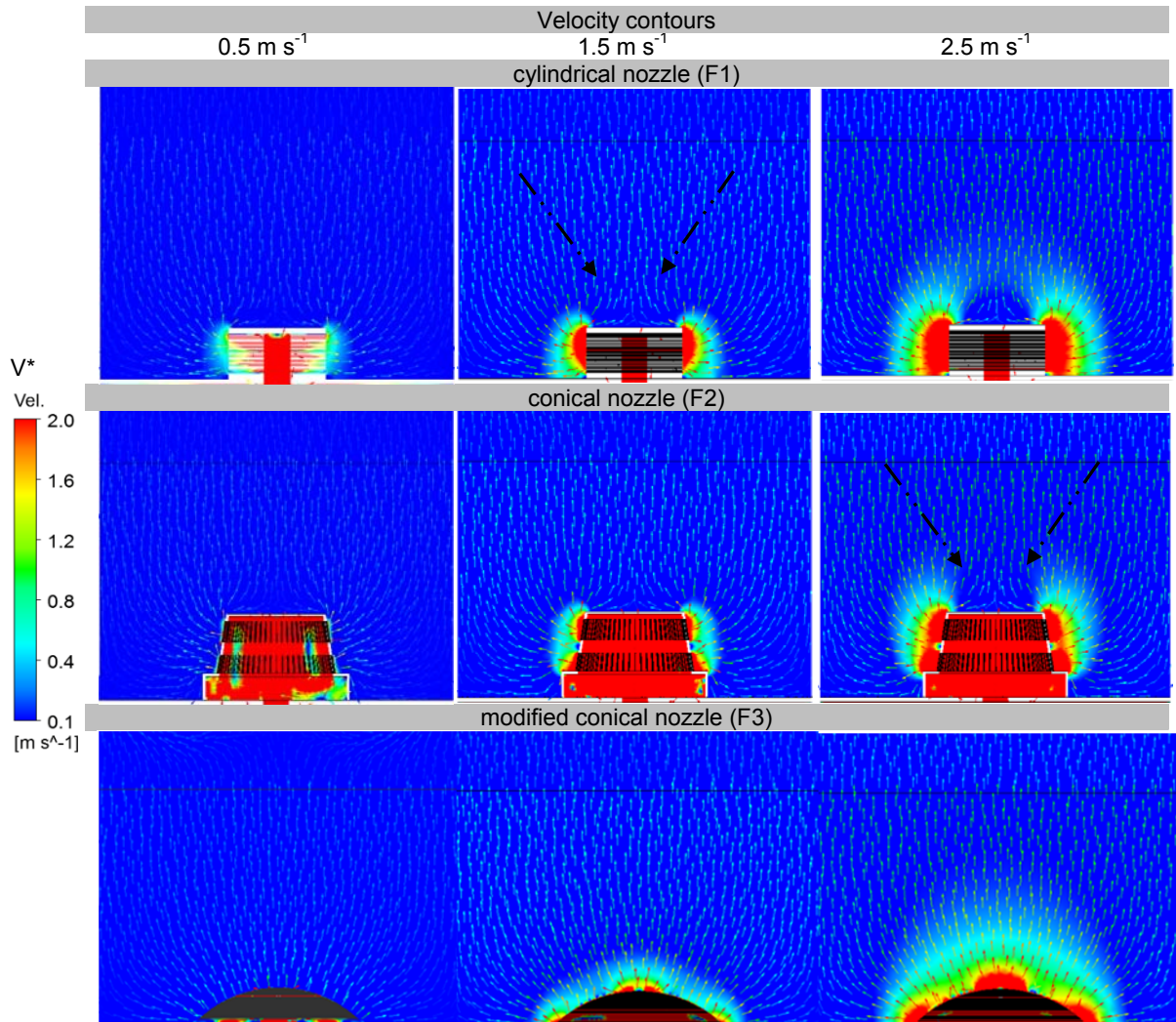

Figure 4: Contour plots of velocity vectors in the direction coincident with the backwash process. Where: [V] velocity vectors legend*

When analyzing the flow profile of the modified nozzle, it is possible to observe that the flow profile of the fluid was predominantly perpendicular, without no stagnation regions. The proposed model distributes the flow uniformly in every action radius, which will provide an equal fluidization throughout the filter internal area.

After analyzing the simulations results, modified conical nozzle prototypes were constructed and submitted to experimental tests to evaluate the filter layer expansion efficiency in backwash process. In the experimental trials, the aimed was to identify the minimum fluidization velocity (Vmf), which shows the transition moment between the static bed (fixed) and moving bed regime (when the first sand particles started the upward movement together with the upper part of the layer). In addition, the aimed was to evaluate the fluidized bed velocity, in expansion of 25% in relation to the static state. Three sand particle sizes intervals were used (0.5 to 1.0 mm, 0.8 to 1.2 mm and 1.0 to 1.5 mm), called by G1, G2 and G3, respectively.

Table1: Minimum fluidization velocity and fluidized bed (expansion of 25%) for three nozzle models.

Flow regimes	G1 Velocity (m s^{-1})			G2 Velocity (m s^{-1})			G3 Velocity (m s^{-1})		
	F1	F2	F3	F1	F2	F3	F1	F2	F3
V$_{mf}$	0.008	0.01	0.007	0.016	0.015	0.011	0.02	0.02	0.015
Fluidized	0.025	0.023	0.018	0.037	0.031	0.020	0.043	0.033	0.030

[F1] cylindrical model, [F2] conical model, [F3] modified conical model

Results were compared with Salcedo (2010), F1 and F2, and it was verified that the projected drains showed decreases the superficial velocity values to reach different flow regimes during the backwash. With the reduction of velocity values, the filter bed washing will depend less on the pumping system and, consequently, would provide more flow to the irrigation system during the backwash inversions of some equipment, thus maximizing efficiency of the filter set used. Additionally, it is believed that with the bed homogenization there will be greater efficiencies in the cleaning of the filter bed, because it allows a greater probability of friction between sand grains and detachment of impurities from the particles and, consequently, longer durations in the filtration time. In agreement with Salcedo's (2010) statement, when he pointed out that the optimal functioning of the filters in the backwash process depends on the layer homogeneity lifting from the beginning of the minimum fluidization, which will affect the effective cleaning of both the surface and depth of the sand layer.

4. Conclusions

The structural models of the nozzle, cylindrical and conical, distributed irregularly the water flow lines and presented stagnation points to the flow. The distribution profile presented by these drains contribute to the reduction of the effective area to the drainage process during the downward flow and bed fluidization during backwash process.
The modified conical nozzle presented satisfactory results, with homogeneous and perpendicular distribution, without stagnation points.

Acknowledgement

References

ANSYS, INC., 2009, CFX-12 User's Guide.

Arbat, G., Pujol, T., Puig-Bargués, J., Duran-Ros, M., Barragán, J., Montoro, L., Ramirez de Cartagena, F. 2011. Using computational fluid dynamics to predict head losses in the auxiliary elements of a microirrigation sand filter. Transactions of the ASABE, v.54, n.4, 1367–1376.

de Deus, F. P. Testezlaf, R. Mesquita, M., 2016, Assessment methodology of backwash in pressurized sand filters. R. Bras. Eng. Agríc. Ambiental, v.20, n.7, p.600-605.

Burt, C. M., 2010, Hydraulics of commercial sand media filters tanks used for agricultural drip irrigation: criteria for energy efficiency. Irrigation Training and Research Center ITRC. Report N. R10-001 September.

Fortuna, A. O., 2000, Técnicas computacionais para dinâmica dos fluidos: conceitos básicos e aplicações. 1ª ed., São Paulo: Editora da universidade de São Paulo, 426p.

Mesquita, M.; Testezlaf, R.; Ramirez, J.C.S., 2012, The effect of media bed characteristics and internal auxiliary elements on sand filter head loss. Agricultural Water Management, v.115, p.178-185.

Salcedo, J. C. R., Efeito das características granulométricas e da altura da camada filtrante no processo de retrolavagem em filtros de areia. 2010, 159 f. Dissertação (Mestre em Engenharia Agrícola) - Faculdade de Engenharia Agrícola, Universidade Estadual de Campinas, Campinas.

Salcedo, J.C.; Testezlaf, R.; Mesquita, M., 2011, Processo da retrolavagem em filtros de areia usados na irrigação localizada. Engenharia Agrícola, v.31, n.6, p.1226-1237.

Santos, M. B., Mesquita, M., Testezlaf, R., 2013, Aplicação de túnel de vento na avaliação de linhas de fluxo geradas por crepinas de filtros de areia. Engenharia Agrícola, v.33, n.3, p. 548-559.

Testezlaf, R.; de DEUS, F. P.; Mesquita, M., 2014, Filtros de areia na irrigação localizada. Campinas (SP): Unicamp, 66p.